THE JOURNAL OF BIOLOGICAL CHEMISTRY
Vol. 274, No. 23, Issue of June 4, pp. 16311–16319, 1999

Printed in U.S.A.

Molecular Cloning and Characterization of a Mouse Homolog of Bacterial ClpX, a Novel Mammalian Class II Member of the Hsp100/Clp Chaperone Family*

(Received for publication, January 28, 1999, and in revised form, March 22, 1999)

Sandro Santagata‡§, Debika Bhattacharyya‡, Fu-Hou Wang‡, Netai Singha‡¶, Andrew Hodtsev‡†, and Eugenia Spanopoulou‡¶‖†

From the Mount Sinai School of Medicine, ‡Ruttenberg Cancer Center, ¶Howard Hughes Medical Institute, New York, New York 10029

In this paper, we present the molecular cloning and characterization of a murine homolog of the *Escherichia coli* chaperone ClpX. Murine ClpX shares 38% amino acid sequence identity with the *E. coli* homolog and is a novel member of the Hsp100/Clp family of molecular chaperones. ClpX localizes to human chromosome 15q22.2–22.3 and in mouse is expressed tissue-specifically as one transcript of ~2.9 kilobases (kb) predominantly within the liver and as two isoforms of ~2.6 and ~2.9 kb within the testes. Purified recombinant ClpX displays intrinsic ATPase activity, with a K_m of ~25 μM and a V_{max} of ~660 pmol min^{-1} μg^{-1}, which is active over a broad range of pH, temperature, ethanol, and salt parameters. Substitution of lysine 300 with alanine in the ATPase domain P-loop abolishes both ATP hydrolysis and binding. Recombinant ClpX can also interact with its putative partner protease subunit ClpP in overexpression experiments in 293T cells. Subcellular studies by confocal laser scanning microscopy localized murine ClpX green fluorescent protein fusions to the mitochondria. Deletion of the N-terminal mitochondrial targeting sequence abolished mitochondrial compartmentalization. Our results thus suggest that murine ClpX acts as a tissue-specific mammalian mitochondrial chaperone that may play a role in mitochondrial protein homeostasis.

The Hsp100/Clp family of ATPases constitutes a group of molecular chaperones that participate in a broad range of biological processes in both prokaryotes and eukaryotes. Sequence similarity and conservation of structural features among the over 70 known family members define two classes, which are further subdivided into eight subfamilies (1). All Hsp100/Clps examined have been demonstrated to assemble into homo-oligomeric ring-shaped structures and to modulate substrates in an ATP-dependent manner (1, 2). Specific substrate recognition occurs through protein-protein interactions directed by the PDZ-like domains of the Hsp100/Clp family members (3). Members of the family participate in the disaggregation of improperly folded and damaged proteins, the facilitation of DNA transposition, the selective coordination of substrate degradation, the regulation of the inheritance of prion-like factors, and the modulation of gene expression (reviewed by Schirmer *et al.* (1)). Despite the involvement of Hsp100s in such diverse processes, it is the conserved structural organization of the members that suggests that these varied functions may involve a common mechanism governing disassembly of high-order quartenary protein complexes (1, 4–6).

E. coli ClpX is a heat-shock protein (7–9) of the class II Hsp100/Clp subfamily (1) and can act alone as a molecular chaperone. It is an essential component of the Mu transposase life cycle where it mediates dissociation of stable MuA tetramer-DNA complexes (10, 11). Deletion of ClpX blocks the growth of Mu by arresting transposition at the transition between the recombination and DNA replication stages (10–12). The molecular chaperone properties of *E. coli* ClpX are further supported by its capacity to prevent the heat inactivation of the bacteriophage λO replication protein, to dissociate preformed λO aggregates, and to stimulate the binding of λO to *ori*λ DNA (13).

While *E. coli* ClpX can function alone as a *bona fide* molecular chaperone, it also contributes to a number of processes as a regulatory subunit of the broad specificity, energy-dependent protease ClpP. In *E. coli*, ClpX and ClpP are translated from a single heat-shock-inducible transcript in accordance with their involvement in stress tolerance (7–9). In this two-component chaperone-protease system, ClpX does not refold proteins to mediate functional reactivation but rather utilizes its chaperone activity to selectively target specific substrates for degradation by channeling them into the proteolytic chamber of the two-ring ClpP tetradecamer. Negative staining electron microscopy (14) and crystallographic analysis of ClpP (15) reveal a structural organization that is homologous to that of the eukaryotic 26 S proteasome. Specific targets of ClpX/P include λO (7, 16), starvation sigma factor (σ^S) (17), SsrA-tagged proteins generated from defective mRNAs (18), the Phd protein of plasmid prophage P1 (19), the *Caulobacter crescentus* cell cycle regulator CtrA protein (20, 21), MuA (22), and the Mu repressor protein (23, 24). Many of these substrates possess 7–11 amino acid C-terminal peptides that are required for recogni-

* This work was supported by Department of the Army/Department of Defense Breast Cancer Predoctoral Training Grant DAMD17-94-J-4111 (to S. S.) and National Institutes of Health Grant 1RO1 AI40191-02 (to E. S.). Confocal laser scanning microscopy was performed with the guidance of Scott Henderson at Mount Sinai School of Medicine Confocal Laser Scanning Microscopy core facility, supported with funding from National Institutes of Health Shared Instrumentation Grant 1 S10 RR0 9145-01 and National Science Foundation Major Research Instrumentation Grant DBI-9724504. The costs of publication of this article were defrayed in part by the payment of page charges. This article must therefore be hereby marked "*advertisement*" in accordance with 18 U.S.C. Section 1734 solely to indicate this fact.

This paper is dedicated to the memory of Andrew Hodtsev and Eugenia Spanopoulou.

† Our mentors, Andrew Hodtsev and Eugenia Spanopoulou, who were the motivating inspiration behind this work, were tragically killed during the crash of Swiss Air Flight 111 on September 2, 1998.

The nucleotide sequence(s) reported in this paper has been submitted to the GenBank™/EBI Data Bank with accession number(s) AF134983.

§ To whom correspondence should be addressed: Mount Sinai School of Medicine, Ruttenberg Cancer Center, 1425 Madison Ave., East Bldg., Box 1130, New York, NY 10029. Tel.: 212-659-5525; Fax: 212-849-2446; E-mail: santas01@doc.mssm.edu.

‖ Assistant investigator in the Howard Hughes Medical Institute and a Cancer Research Institute Clinical Investigator.

tion by the PDZ-like domains of ClpX (3).

While prokaryotes possess pan-cellular chaperone distribution, eukaryotes require compartment-specific chaperones to negotiate and maintain polypeptide chains within the appropriate tertiary structure and to facilitate the degradation of unsalvageable or transient protein molecules and complexes (25, 26). As expected from the proposed endosymbiotic origins of the mitochondria (27, 28), the molecular chaperones that direct mitochondrial function display significant sequence homolog to bacterial counterparts. In particular, mitochondrial proteins Hsp70, chaperonins Hsp60/Hsp10 and Hsp78 are homologous to *E. coli* DnaK, GroEL/GroES, and the class I Hsp100/Clp family, respectively. The conspicuous absence of a eukaryotic homolog of the ClpX class II Hsp/Clp subfamily was remedied following the sequencing of the complete genome of *Saccharomyces cerevisiae* (29, 56) and the subsequent demonstration that the gene product termed Mcx1p partitioned to the mitochondria (30). However, a mammalian homolog had remained until this point unidentified. The existence of such a member has been strongly implied by the cloning of a human homolog of ClpP that sorts to the mitochondrial matrix (31, 32).

In this report, we describe the identification and initial characterization of murine ClpX, a novel mammalian member of the Hsp100/Clp family of molecular chaperones that displays distinct sequence similarity with its *E. coli* counterpart. We demonstrate that murine ClpX is directed to the mitochondria by an N-terminal targeting peptide. In line with its likely role as a mitochondrial molecular chaperone, we show that ClpX possesses an intrinsic ATPase activity that is resilient *in vitro* to fluctuations in reaction conditions reflecting environmental stress. Its capacity to interact with mouse ClpP in mammalian overexpression experiments suggests that mouse ClpX/P may represent a novel system for the regulation of mitochondrial protein homeostasis.

EXPERIMENTAL PROCEDURES

Cloning of the Murine Homolog of Bacterial ClpX, Chromosomal Localization, and Tissue Expression—Blast searches of the data base of expressed sequence tags (dBEST) (33) using *E. coli* ClpX revealed the partial murine ClpX EST clone Aa013832 (Image Consortium clone 441677). This ClpX fragment was random prime [α-^{32}P]dCTP-labeled with Klenow fragment and used to screen a mouse keratinocyte library BALB/MK (34). Full-length murine ClpX in pCEV27 was identified (pM11/18) and nucleotide sequence was obtained by automated sequencing of both strands (Utah State University Biotechnology Center). A human chromosomal location of ClpX was assigned by analyzing the physical map of the human genome available at *http://www.ncbi.nlm.nih.gov/genemap/* (35, 36). A mouse Multiple Tissue Northern (CLONTECH) was hybridized as recommended by the manufacturer with an [α-^{32}P]dCTP body-labeled PCR[1] fragment generated using primers 467 (5′-ATGTTAGGAAGACTGGGGACG-3′) and 238 (5′-TTATAATGATTATACACGGC-3′). The C terminus of proteins were considered homologous to the C-terminal targeting sequence of bacterial ClpX substrates if all four of the following criteria were fulfilled: 1) the final two amino acids were nonpolar, 2) the preceding 7 amino acids were preferentially polar or charged, 3) at least 6 of the 11 amino acids were similar to the final amino acids of the SsrA tag (18), and 4) at least 1 of the first 2 amino acids was nonpolar.

Construction of ClpX in Vitro Transcription-Translation and Mammalian Expression Vectors—To create serial N-terminal deletions of ClpX in the Sp6 promoter driven vector pCEV27, PCR products bearing optimal Kozak translation start sequences were cloned between *Bam*HI of the polylinker and an *Ava*I site internal to ClpX (pCEV27ClpXM$_1$, pCEV27ClpXM$_2$, pCEV27ClpXΔ65). To generate fusions to the C terminus of glutathione *S*-tranferase of the N-terminal serial deletions, *Bam*HI fragments from the start ATG to internal to the 3′-untranslated region (nt 2439) were subcloned from the pCEV27 vectors into the eIF2 promoter driven mammalian expression vector pEBG (37) (pEBGClpXM$_1$, pEBGClpXM$_2$, and pEBGClpXΔ65). The mutation of K300A was introduced with a mutated PCR oligonucleotide and the fragment was subcloned between *Ava*I (nt. 628) and *Xba*I (nt 1341) (pEBGClpXM$_2$K300A). Red-shifted green fluorescent protein fusions in the mammalian expression vector pEGFPN3 (CLONTECH) were generated by PCR amplification from the *Apa*LI site (nt 1853) to the C terminus, which was fused in frame with the N terminus of EGFP using the *Kpn*I site. The N terminus of ClpX was inserted simultaneously as a *Bam*HI-*Apa*LI fragment using the 5′ polylinker site *Bgl*II (pClpXEGFPM$_1$, pClpXEGFPM$_2$, and pClpXEGFPΔ65). The mouse homolog of ClpP (GenBank™ accession number AJ005253) was amplified by PCR from the mouse keratinocyte library BALB/MK. The fragment spanning the nucleotides coding for amino acids 56–272 (with a deletion of the first 55 N-terminal amino acids, which are proteolytically removed in mature ClpP) was fused in frame with a C-terminal HA tag (amino acids:YPYDVPDYA) in the eIF2 promoter vector pEBB (pEBBClpPΔ55 3′-HA). All PCR-generated constructs were confirmed by sequencing.

Cell Culture and Recombinant Eukaryotic Protein Expression—The human embryonic kidney fibroblast line, 293T, was grown in Dulbecco's modified Eagle's medium containing 5% fetal bovine serum at 37 °C in a 5% CO_2 atmosphere. GST fusion proteins of ClpX were overexpressed from the pEBG vector (see above) by transient transfection of 293T cells at 25% confluence using the calcium phosphate precipitation method. Cells were harvested 48 h post-transfection and processed as described previously (38) and dialyzed in 25 mM Tris, pH 8.0, 200 mM NaCl, 2 mM EDTA, 10 mM β-mercaptoethanol, and 20% glycerol. Protein quantitation was conducted following SDS-PAGE and Coomassie staining using dilutions of bovine serum albumin as a standard.

ATPase and Nucleotide Binding Assays—Indicated concentrations of recombinant GSTClpX wild-type and mutant proteins were incubated in a 20-μl reaction with 25 mM Tris, pH 7.4, 10 mM $MgCl_2$, 1 mM dithiothreitol, BSA 0.1 μg/μl, 1–500 μM ATP, and 0.5 μl of [α-^{32}P]ATP (3.3 μM; 3000 Ci/mM, Amersham Pharmacia Biotech) at 37 °C for indicated times. Reactions were stopped by the addition of 25 mM EDTA and freezing at −70°C. ½0th of the reaction volume was spotted onto thin layer chromatography (TLC) plates (polyethyleneimine cellulose F; EM Science), and separation of P_i from ATP was attained in 1.0 M formic acid and 0.5 M $LiCl_2$. Following autoradiography, quantitation of hydrolyzed ATP was determined by Molecular Analyst phosphoimaging (Bio-Rad). Nucleotide binding studies (39) were performed in 20-μl binding reactions with 25 mM Tris, pH 7.4, 10 mM $MgCl_2$, 1 mM dithiothreitol, 0.1 μg/μl BSA, 0.33 μM [α-^{32}P]ATP (3,000 Ci/mM and 3.3 μM) and 0.1 μM wild-type or mutant GSTClpX protein for 10 min at 4°C. Free nucleotides were removed with G-50 Sephadex spin columns (Roche Molecular Biochemicals), collected in tubes containing 5 μl of 500 mM EDTA, pH 7.5, and placed immediately on dry ice to stop the reaction. Bound nucleotides in the spin-through were quantitated on a Beckman LS 6500 scintillation system and the ratio of ADP/ATP in the flow-through was determined following separation of an aliquot of the spin-through by TLC. Following autoradiography, values were derived by phosphoimaging.

ClpX/ClpP Protein Interaction—Recombinant proteins, GSTClpX full-length or N-terminal truncations in pEBG, and 3′-HA-tagged ClpP in pEBB were transiently overexpressed in immunoprecipitation cells using calcium phosphate precipitation. Cells were harvested in phosphate buffered saline (PBS) 48 h post-transfection and freezed-thawed once at room temperature. Cells were resuspended in immunoprecipitation lysis buffer containing 20 mM Tris, pH 8.0, 150 mM NaCl, 0.5% Nonidet P-40, 10% glycerol, 1 mM phenylmethysulfonyl fluoride, 0.1 μM aprotinin, 1 μM leupeptin, and 1 μl of pepstatin and sonicated extensively. The lysate was cleared in a microcentrifuge for 15 min at 14,000 rpm and 4 °C. An aliquot was removed for protein expression evaluation, and the remainder of the lysate was incubated on glutathione beads for 2 h at 4 °C with gentle rocking. The beads were washed five times with mild vortexing in immunoprecipitation lysis buffer and finally resuspended in 2 × SDS-PAGE loading buffer. The interaction was subsequently evaluated with Western analysis.

Cellular Localization of Recombinant ClpX—10 μg of pEGFPN3, pClpXM$_1$EGFP, pClpXM$_2$EGFP, or pClpXΔ65EGFP were transiently transfected in 293T cells as described above. Thirty-six hours post-transfection, the cells were incubated with 1 μM Mitotracker® Red CMXros (Molecular Probes) for 2 h at 37 °C. Cells were rinsed once in PBS prewarmed to 37 °C, incubated for 20 min in 4% paraformaldehyde, rinsed three times in room temperature PBS, fixed for 15 min in cold methanol/acetone (1:1), and rehydrated in PBS for 10 min. Follow-

[1] The abbreviations used are: PCR, polymerase chain reaction; nt, nucleotide(s); HA, hemagglutinin; GST, glutathione *S*-transferase; PAGE, polyacrylamide gel electrophoresis; BSA, bovine serum albumin; PBS, phosphate-buffered saline; EST, expressed sequence tag; GFP, green fluorescent protein; EGFP, enhanced GFP; CTS, C-terminal targeting sequence.

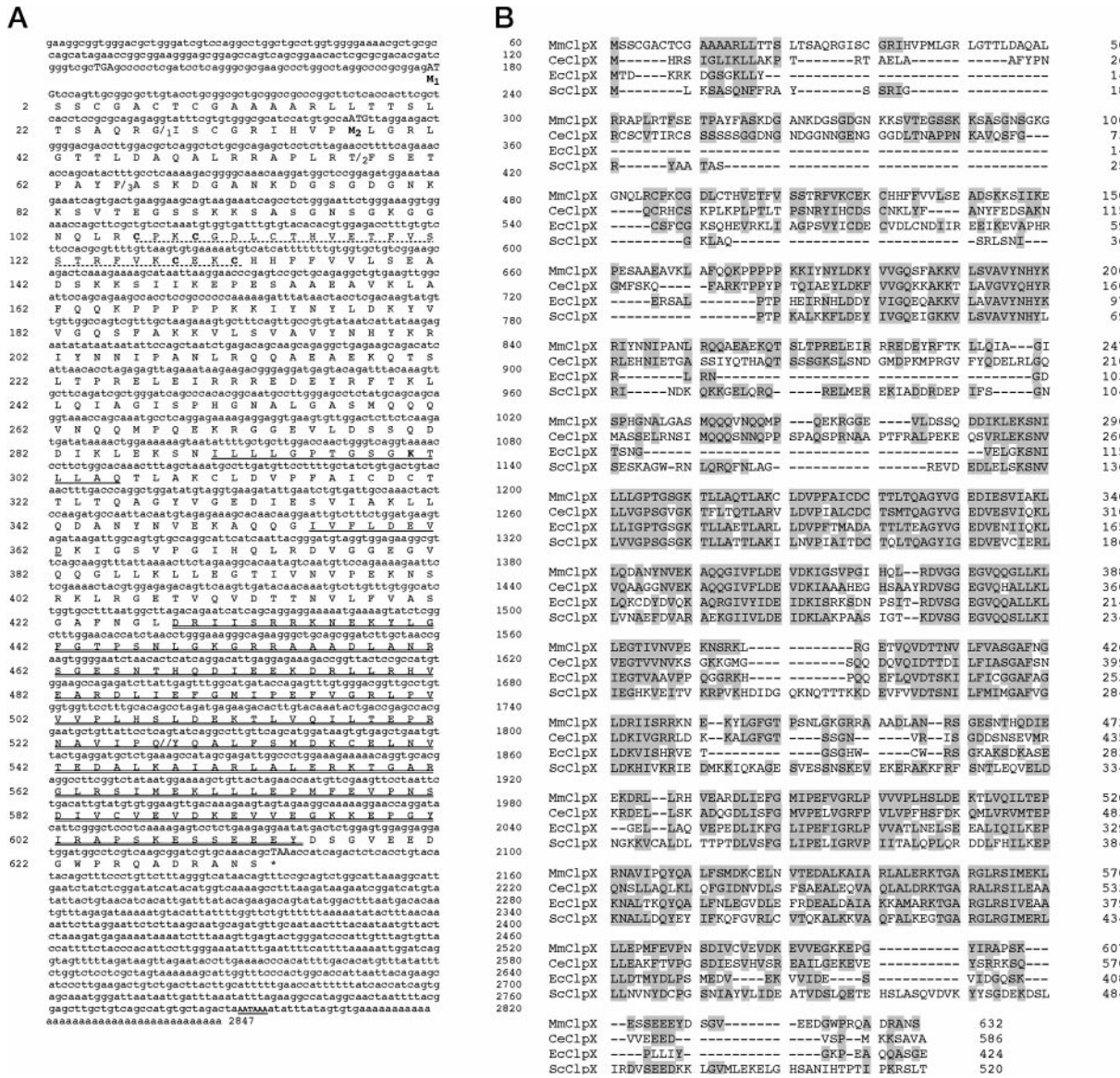

FIG. 1. **cDNA and deduced amino acid sequence of murine ClpX indicating evolutionary conservation of protein domains.** *A*, the cDNA and protein sequences of murine ClpX are displayed. Putative translation initiation and stop codons are emphasized in *uppercase letters*. Two possible start methionines are indicated (M_1 and M_2) in *bold* and the three consensus cleavage sites ($/_1$ of the R-2 motif and $/_2$ and $/_3$ of the R-10 motif) (42) for the matrix processing peptidase are marked. The predicted C4-zinc finger is *underlined by dots* with the putative Zn^{2+} coordinating cysteines highlighted in *bold*. The P-loop and Walker B sites of the ATPase motif are *single underlined* with lysine 300 of the GKT motif indicated in *bold*. The region displaying homology to PDZ domains is *double underlined* with the boundary between PDZ domain A and B demarcated by a //. The polyadenylation consensus is *single underlined* and in *small caps*. *B*, protein sequence alignment of mouse, *C. elegans* (GenBank™ accession number Z73906), *E. coli* (GenBank™ accession number Z23278), and *S. cerevisiae* (GenBank™ accession number Z36096) ClpX with areas of similarity *shaded*. Percentage amino acid identity and similarity reported in the text were calculated using the putative mature form of mouse ClpX cleaved after the first 65 amino acids.

ing three washes in PBS + 1% BSA, the cells were incubated for 10 min at room temperature with 5 μg/ml 4′,6′-diaminidino-2-phenylindole (Sigma) in PBS + 1% BSA. Following three washes in PBS + 1% BSA, the coverslips were mounted. Images were acquired using confocal laser microscopy.

RESULTS

Isolation of a Murine Homolog of Bacterial ClpX and Evolutionary Conservation of Functional Domains—Due to our laboratory's interest in the remodeling of higher order nucleoprotein complexes in mammalian transposition and recombination reactions, we screened the data base of expressed sequenced tags (dBEST) (33) for a mouse homolog of the *E. coli* ATP-dependent remodeling factor ClpX. Identification of EST clone Aa013832 permitted isolation of a full-length cDNA of 2847 base pairs encoding mouse ClpX (Fig. 1*A*) from a keratinocyte library. The potential open reading frame is demarcated by two stop codons, a 5′ TGA (nt 128–130) and a 3′ TAA (nt 2075–2077), which contain two possible sites of translation initiation, ATG1 (nt 179–181: M_1) and ATG2 (nt 287–289: M_2). From ATG1, the cDNA comprises an open reading frame of 1896 base pairs and encodes a predicted protein of 632 amino acids with a molecular mass of 69,174 Da and a theoretical isoelectric point of 7.76. The mouse ClpX as compared with *Caenorhabditis elegans*, *E. coli*, and *S. cerevisiae* ClpX demonstrates 40, 38, and 32% amino acid identity and 59, 46, and 48% similarity, respectively (Fig. 1*B*). A consensus polyadenylation site (AATAAA) is located 14 base pairs before the 3′ poly(A) start (Fig. 1*A*).

Functional analysis of mouse ClpX is dependent upon an understanding of its component motifs. We thereby note that the primary structure of the 69-kDa mouse ClpX polypeptide displays three discernable domains that are evolutionary con-

served through *E. coli* (Fig. 1, *A* and *B*). First, along with the *C. elegans* and *E. coli* homologs, murine ClpX possesses toward the N terminus a C4-type zinc finger (amino acids 106–131) of unknown function. Second, ClpX bears a characteristic ATPase motif with a classic P-loop (amino acids 290–305) and Walker B Mg^{2+} binding pocket (amino acids 355–362) with distinct similarity to those of the F_1-ATPase and P-type transporters (40). Third, the C terminus contains two tandem PDZ-like domains, which display 44, 31, and 41% identity and 65, 58, and 58% similarity with the PDZ-like domains of *C. elegans*, *S. cerevisiae*, and *E. coli*, respectively. In *E. coli*, these domains mediate specific substrate recognition (3). In addition to these three highly conserved motifs, mouse ClpX possesses at the N terminus an apparent mitochondrial targeting sequence (41–43) spanning as much as the first 65 amino acids of the protein (Fig. 1*A*). This region is characterized by the predicted capacity to form an amphiphilic helix coupled with a biased distribution of positively charged amino acids (7 arginines), an abundance of hydroxylated residues (13 serines or threonines), and a paucity of negatively charged amino acids (1 aspartate and 1 glutamate). Maturation of the ClpX preprotein can be predicted to result following cleavage by the mitochondrial processing peptidase at three putative sites, one site within an R-2 motif and another two sites within an R-10 motif (Fig. 1*A*) (42, 43).

To determine whether translation preferentially initiates at AUG 1 or 2, the migration was compared between full-length ClpX cDNA *in vitro* translation products and the products from truncated forms of ClpX starting from either ATG1 ($ClpXM_1$), ATG2 ($ClpXM_2$), or an N-terminal deletion of the first 65 amino acids (ClpXΔ65) (Fig. 2*B*). While over 98% of the translation products from the full-length cDNA (Fig. 2*B, arrow a* in *lane 1*) co-migrated with $ClpXM_1$ (*lane 2*), a minor species was produced (*arrow b* in *lane 1*) that co-migrated with the $ClpXM_2$ product (*lane 3*). The preponderance of initiation at AUG1 suggests that this is the biologically relevant start site. However, while translation initiation at AUG2 may be specific to the *in vitro* transcription/translation system and may not occur *in vivo*, the possibility that the two translation isoforms are targeted differentially to separate subcellular compartments lead us to characterize both start forms in subsequent studies.

Tissue-specific Expression and Assignment of Chromosomal Localization—Northern blot analysis was used to study the tissue distribution of ClpX encoding mRNA. Samples of poly(A)$^+$ RNA from eight different BALB/c mouse tissues were hybridized with labeled probe specific for ClpX (Fig. 2*A*). The relative expression level is highly variable between different tissues. ClpX was expressed predominantly in the liver as a single transcript of ~2.9 kb and in the testes as two transcripts of ~2.6 and ~2.9 kb. The length of the 2.9-kb mRNA corresponds to the size of the full-length cDNA (Fig. 1*A*). The two mRNAs in the testes may result from alternative RNA splicing. Lower expression of the 2.9-kb ClpX transcript was detected in the heart and kidney. Very low levels were observed in skeletal muscle (upon overexposure) with no apparent expression detectable in the brain, spleen, and lung.

Human chromosomal localization of ClpX was assigned using the Gene Map of the Human Genome, which is a physical map of cDNA-based sequence-tagged sites (35, 36) available on the World Wide Web. This resource of currently 30,181 genes utilizes the unique 3′-untranslated region of a cDNA to position ESTs relative to microsatellite markers by radiation hybrid mapping with an error rate of 1.08%. ClpX was typed on a Genebridge4 radiation hybrid panel using PCR primers designed to the 3′-untranslated region of the human gene and determined to map to chromosome 15q22.2–22.3 between fixed reference markers D15S125 and D15S216.

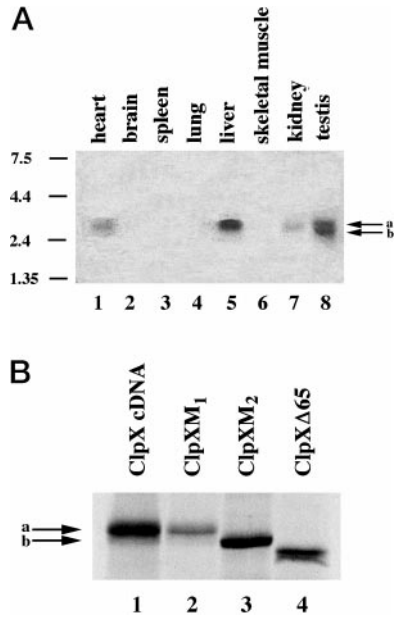

FIG. 2. **Northern blot analysis of mouse poly(A)$^+$ RNA from a multiple tissue Northern blot and initiation codon usage analysis by *in vitro* transcription-translation.** *A*, a multiple tissue Northern blot (CLONTECH) of poly(A)$^+$ RNA from BALB/c mouse heart (*lane 1*), brain (*lane 2*), spleen (*lane 3*), lung (*lane 4*), liver (*lane 5*), skeletal muscle (*lane 6*), kidney (*lane 7*), and testis (*lane 8*) was probed with a ^{32}P-body-labeled PCR product spanning nucleotides 287–777. *Numbers* on the *left* indicate sizes in kilobases. *B*, [^{35}S]methionine-labeled forms of ClpX were generated using a coupled i*n vitro* transcription-translation rabbit reticulocyte lysate system and resolved by SDS-PAGE. *Lane 1* contains translation products (*arrows a* and *b*) from the ClpX full-length cDNA (pM11/18) with the entire reported 5′-untranslated region and both initiation codons ATG1 (M_1) and ATG2 (M_2) intact. Migration can be compared with products initiated directlyfrom either ATG1 in the absence of a 5′-untranslated region (pCEV27$ClpXM_1$) (*lane 2*), from ATG2 (pCEV27$ClpXM_2$) (*lane 3*), or from a deletion of the first 65 amino acids spanning the mitochondrial targeting peptide (pCEV27ClpXΔ65) (*lane 4*).

ATPase Activity of Mouse ClpX—The presence of a consensus ATPase motif (Fig. 1*A*) led us to analyze the kinetics of ATP hydrolysis by ClpX. Overexpressed recombinant ClpX was purified from a human kidney fibroblast cell line, 293T, as a GST fusion protein (Fig. 3A). Titration of GSTClpXΔ65 (Fig. 3*B*) and a time course of P_i release (Fig. 3*C*) revealed linear kinetics in the presence of 0.05 μM ClpX over an incubation of 5–10 min. These conditions were used for all subsequent assays. ClpX hydrolyzed ATP with a K_m of ~25 μM and a V_{max} of ~660 pmol min^{-1} μg^{-1}, which corresponds to the hydrolysis of ~1 molecule of ATP/molecule of ClpX/s (Fig. 3*D*). All three fusions shown in Fig. 3*A* display equivalent reaction kinetics. When the ATPase activity of ClpX was tested at 150 mM NaCl to more closely resemble physiological ionic strength, the K_m was essentially unchanged (data not shown). Either Mg^{2+} or Mn^{2+} was required for efficient ClpX ATPase activity. Like ClpA and ClpB, ClpX retained partial ATPase activity in Ca^{2+}. Unlike Hsp104, which hydrolyzes ATP in Co^{2+} and Ni^{2+} (4), ClpX demonstrated negligible activity using these divalent cations (Table I).

To demonstrate that the ATPase activity is intrinsic to ClpX, lysine 300 of the P-loop motif was replaced by alanine (K300A) (Fig. 4*A*, *lane 4*). Consonant with the role of this lysine in other ATPases as an integral structural component of the P-loop and a point of coordination for the β- and γ-phosphates of bound nucleotides (44), the mutation entirely abolished detectable ClpX mediated ATPase activity (Fig. 4*B*). Next, the effect of the mutation on nucleotide binding was evaluated to determine whether the deficiency in hydrolysis resulted from inability to

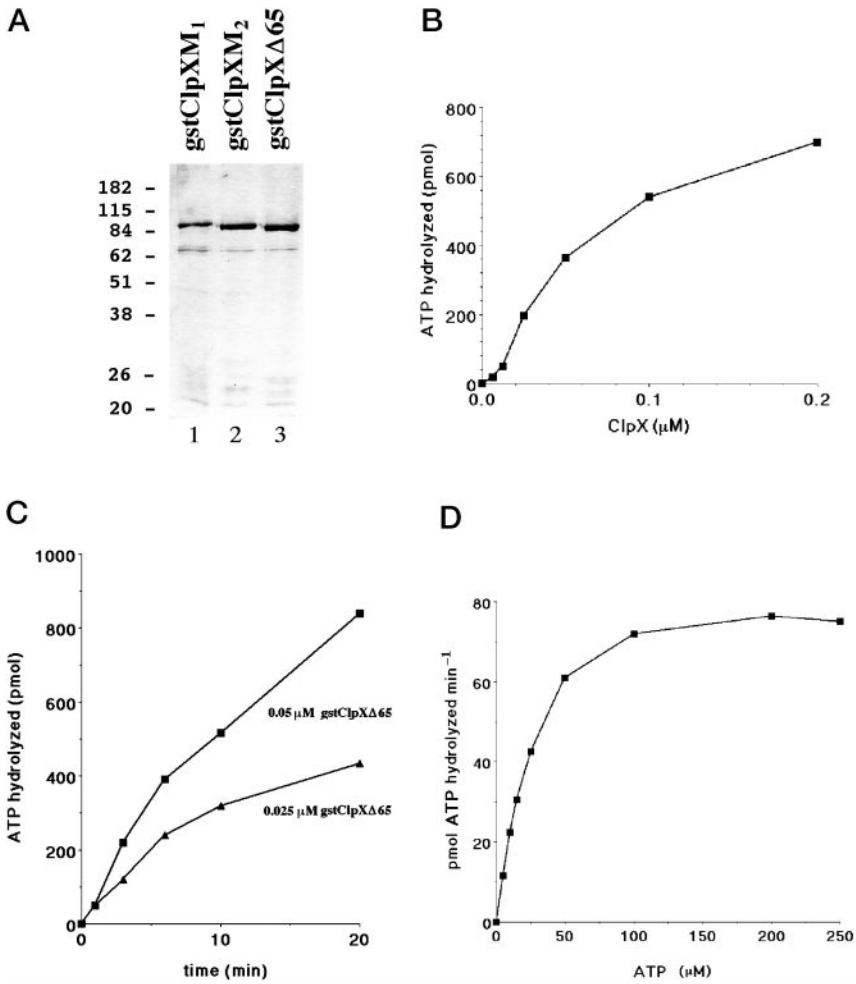

FIG. 3. **Characterization of the ATPase activity of murine ClpX.** *A*, SDS-PAGE analysis of GSTClpXM$_1$ (*lane 1*), GSTClpXM$_2$ (*lane 2*), and GSTClpXΔ65 (*lane 3*) purified following transient overexpression in 293T cells. *B*, picomoles of ATP hydrolyzed *versus* concentration of ClpX. The amount of ATP hydrolyzed in 6 min at 37 °C by increasing amounts of GSTClpXΔ65 (0.006–0.2 μM) in reactions containing 1000 pmol ATP (50 μM final ATP concentration) was determined. P_i was separated from unhydrolyzed ATP by thin layer chromatography, and amounts were quantitated following autoradiography. *C*, time course of ATPase activity; picomoles of ATP hydrolyzed at 37 °C over time (minutes) by 0.05 and 0.025 μM GSTClpXΔ65 with 1000 pmol ATP (50 μM) as the initial substrate amount. *D*, rate of hydrolysis was determined from the picomoles of P_i released over 6 min by 100 ng of ClpX (0.05 μM). K_m and V_{max} values were also derived from a Lineweaver-Burk plot of the same values (graph not shown). Reaction rates were calculated using 0.05 μM GSTClpXΔ65 at initial ATP concentration values of 5, 10, 15, 25, 50, 100, 200, and 250 μM ATP. GSTClpXM$_1$ and GSTClpXM$_2$ yielded similar K_m and V_{max} values.

TABLE I

ATPase activity of ClpX in the presence of various divalent cations

ATPase activity was evaluated with 0.05 μM GSTClpXΔ65 at 37 °C for 6 min with 50 μM initial ATP (1000 pmol) and 10 mM amounts of the indicated divalent cation. No activity was noted in the presence of 10 mM EDTA. The percent activity reported is standardized with hydrolysis in Mg^{2+} as 100%. The divalent ion dependence of other Hsp100/Clp family members has been compiled previously by Schirmer *et al.* (4).

Ion	ClpX	ClpX
	pmol P_i released	%
Mg^{2+}	378 ± 18	100
Mn^{2+}	355 ± 25	94
Ca^{2+}	34 ± 5	9
Zn^{2+}	3 ± 2	0
Fe^{2+}	8 ± 2	2
Co^{2+}	2 ± 2	0
Cd^{2+}	1 ± 2	0
Ni^{2+}	2 ± 2	0

recruit ATP. At 4 °C, wild-type GSTClpXM$_1$, GSTClpXM$_2$, and GSTClpXΔ65 associated with both ATP and ADP (Fig. 4*C*). The ratio of bound ATP to bound ADP was about 1:5. This association required the presence of Mg^{2+} (data not shown). In contrast, GSTClpXΔ65K300A binding to ATP at 4 °C was negligible (Fig. 4*C*), suggesting that Lys^{300} is critical for both ATP binding and hydrolysis.

Both of the two previously cloned members of the Hsp100/Clp family in *S. cerevisiae*, Hsp104 and Hsp78, mediate stress tolerance under conditions of extreme temperature (6, 45), and Hsp104 is also of critical importance for tolerance to ethanol (46). Hence, we analyzed the ATPase profile of ClpX under various conditions reflecting environmental stress (4). Interestingly, ClpX is resilient to varied alterations in reaction conditions. ATP hydrolysis was essentially unaltered over a pH range of 6.8–8.8 (Fig. 5*A*) and decreased only 15% when the salt range was varied from the physiological value of 150–450 mM NaCl (Fig. 5*B*). In addition, ClpX retained 75% of wild-type activity in 20% ethanol (Fig. 5*C*) and 90% of wild-type activity at 55 °C (Fig. 5*D*). The ability to function across a broad scope of reaction parameters suggests that ClpX may function along with the other Hsp100/Clp family members in response to cellular stress.

ClpX Interacts with ClpP—The absence of an open reading frame in the complete yeast genome demonstrating distinct homology to bacterial ClpP (29, 56) suggests the possibility that ClpX may have evolved in eukaryotes to function independently of ClpP. To address whether mouse ClpX could still as-

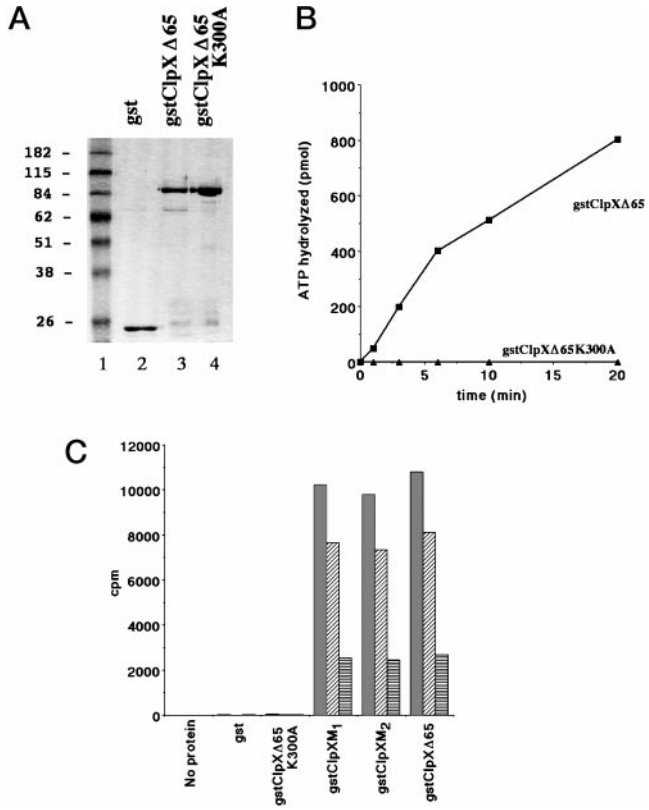

FIG. 4. **ATP hydrolysis and nucleotide binding of P-loop mutation K300A.** *A*, SDS-PAGE analysis of GST, wild-type GSTClpXΔ65, and the P-loop substitution GSTClpXΔ65K300A. *B*, time courses of ATP hydrolysis for reactions containing 0.05 μM GSTClpXΔ65 or 0.05 μM GSTClpXΔ65K300A at 37 °C with 1000 pmol as the initial amount of ATP. *C*, nucleotide binding was assayed by incubating ATPase assay reactions containing 0.05 μM protein at 4 °C for 10 min and removing unincorporated nucleotides with G-50 Sephadex® spin columns. The ADP/ATP ratio of the bound nucleotides was determined following separation by thin layer chromatography for reactions with no protein, GST alone, GSTClpXΔ65K300A, GSTClpXM$_1$, GSTClpXM$_2$, and GST-ClpXΔ65. Total bound nucleotides, bound ADP, and bound ATP for each protein reaction are reported as counts per minute. Experiments were repeated three times with deviations from the mean <10%.

sociate to form a complex with mouse ClpP, we performed co-precipitation assays between N-terminal serial deletions of ClpX fused in frame with the C terminus of glutathione *S*-transferase and ClpP (amino acids 56–272) with a C-terminal HA tag. Recombinant proteins were overexpressed in 293T cells and interaction was evaluated by affinity precipitation of complexes on glutathione beads. GSTClpXM$_1$ does not interact nonspecifically with any anti-HA cross-reactive species in 293T cells not transfected with ClpP3′HA (Fig. 6, *lane 1* in the *middle panel*). GST alone did not interact with ClpP3′HA (Fig. 6, *lane 2* in the *middle panel*). GSTClpXM$_1$, GSTClpXM$_2$, and GSTClpXΔ65 all co-precipitated ClpP3′HA with approximately equal efficiency (Fig. 6, *lanes 3–5* in the *middle panel*). Precipitated levels of the GST and GSTClpX proteins were evaluated by Western analysis (Fig. 6, *upper panel*). Expression levels of ClpP3′HA were assessed by Western analysis of whole cell extracts from the transfected cells (Fig. 6, *lower panel*). As a control, GSTClpX proteins did not interact with various HA-tagged forms of Rag 1 and 2 proteins (data not shown). In all, the data demonstrate the capacity of mouse ClpX/ClpP to form a stable complex. This interaction suggests that mouse ClpX may function analogously to *E. coli* ClpX as an energy-dependent regulator of ClpP function.

Subcellular Sorting of Mouse ClpX-Green Fluorescent Protein Fusions—The presence of an apparent mitochondrial targeting sequence on the N terminus of ClpX strongly suggested that ClpX would localize to the mitochondria along with its interacting partner protein ClpP (31). To explore the intracellular distribution of ClpX, we fused the C terminus of the full-length ClpXM$_1$ preprotein with the N terminus of a red-shifted variant of green fluorescent protein (EGFP). In addition, the possibility that use of the second ATG (M$_2$) might direct differential compartmentalization of this *in vitro* minor translation species (Fig. 2*B*) was explored using a ClpXM$_2$–EGFP fusion initiated directly from the second methionine. The fusions were overexpressed in 293T cells and analyzed using confocal laser scanning microscopy. With EGFP alone, fluorescence was observed throughout the nucleus and cytoplasm (Fig. 7*A*). On the other hand, both the ClpXM$_1$-EGFP and ClpXM$_2$-EGFP fusions generated fluorescence in the form of discrete cytoplasmic rod-like elements, suggesting distribution of ClpX to the paracrystalline structures of the mitochondria (Fig. 7, *B* and *C*). To verify that the punctate staining suggestive of mitochondrial localization was dependent on the integrity of the N-terminal 65-amino acid targeting peptide, we analyzed distribution of ClpXΔ65-EGFP lacking the targeting sequence. Consistent with the existence of an N-terminal mitochondrial targeting peptide, this deletion ablated the punctate fluorescence and, in turn, generated homogenous cytoplasmic staining (Fig. 7*D*). Subcellular compartmentalization of ClpXM$_1$-EGFP to the mitochondria was further supported by co-localization studies using a mitochondrion-selective dye, Mitotracker® Red (Fig. 7, *E–G*), in which co-segregation of the EGFP fluorescence (Fig. 7*E*) with the rhodamine emission of Mitotracker® (Fig. 7*F*) was observed through numerous confocal sections (Fig. 7*G*). Similar co-localization was observed for ClpXM$_2$-EGFP (data not shown).

DISCUSSION

The current study presents the cloning and initial characterization of murine ClpX, a novel member of the Hsp100/Clp family of molecular chaperones and energy-dependent protease regulators. The encoded protein of 632 amino acids is a class II member as characterized by its general structural organization as well as the presence of only one and not two nucleotide binding domains (1). Sequence homology exhibited between the *E. coli*, *S. cerevisiae*, *C. elegans*, and mouse members of this chaperone subfamily is concentrated toward the central and C-terminal regions of the molecules corresponding to the ATPase and the PDZ-like substrate recognition domains. Significant amino acid sequence divergence is observed at the N terminus due to the nonconserved nature of mitochondrial targeting peptides and the obvious absence of the peptide in *E. coli*. An additional N-terminal difference is that only three of the homologs contain a C4-zinc finger, with its noticeable absence in *S. cerevisiae* (Fig. 1*B*). Since a ClpP homolog is also not evident in *S. cerevisiae* (29, 56) the C4-zinc finger of *E. coli*, *C. elegans*, and mouse ClpX is a potential candidate for mediating recruitment of ClpP. However, as is the case with DNA J, the C4-zinc binding domain may also direct recognition and binding of denatured protein substrates (47). It is interesting to speculate that ClpX may possess a bimodal capacity for substrate recognition with the N-terminal C4-zinc finger nonspecifically contacting denatured polypetides and the C-terminal PDZ domains directing specific interactions with native proteins.

Since the molecular chaperone activity of Hsp100/Clp family members has been directly linked to their ability to hydrolyze ATP (13, 48, 49), it is noteworthy that the K_m of basal ATPase hydrolysis by ClpX is ~25 μM. This value is over 20- (low salt) to 200-fold (high salt) lower than that obtained for Hsp104 (4), 20-fold lower than that for *E. coli* ClpX (13), 8-fold lower than

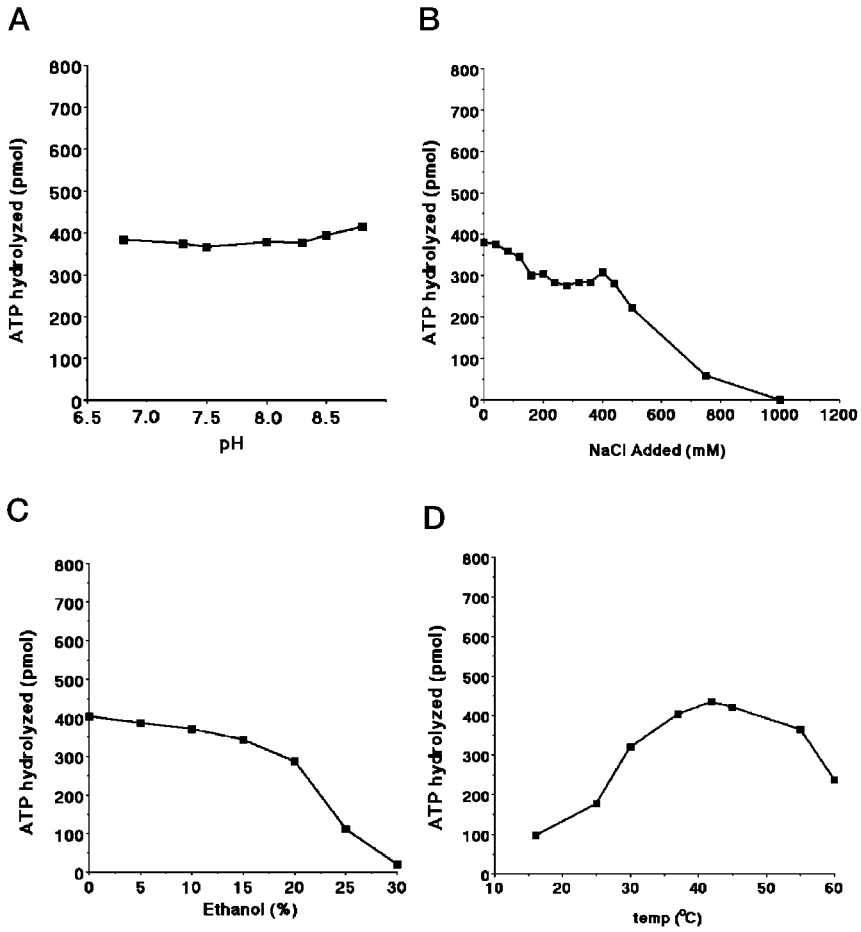

FIG. 5. **ClpX ATPase activity under stress conditions.** The ATPase activity of GSTClpXΔ65 under conditions of varied pH (*A*), salt (*B*), ethanol (*C*), and temperature (*D*). Reactions were conducted at 37 °C for 6 min using 0.05 μM GST-ClpXΔ65 and 1000 pmol of ATP.

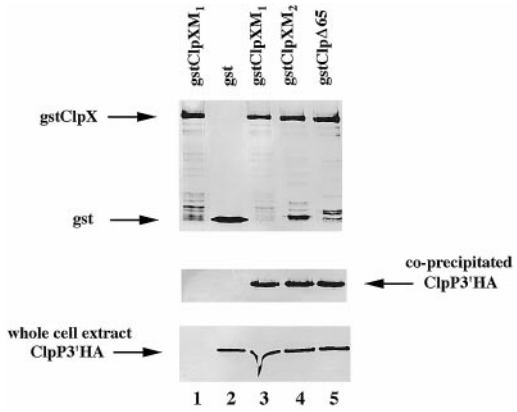

FIG. 6. **Interaction of ClpX and ClpP.** Co-precipitation assays were used to analyze the interaction between wild-type or mutant recombinant GSTClpX proteins transiently expressed in 293T cells with a N-terminally truncated mouse ClpP (Δ55) tagged at the C terminus with an HA peptide. Interaction with ClpP(3′HA) was assayed with GST alone, GSTClpXM$_1$, GSTClpXM$_2$, and GSTClpXΔ65 by co-precipitation with glutathione beads followed by Western analysis. The *upper panel* reveals the amount of GST or GSTClpX fusions precipitated in each lane as monitored by a monoclonal anti-GST antibody. The *middle panel* represents interacting ClpP(3′HA) as detected by a monoclonal anti-HA antibody 12CA5. Expression levels of ClpP(3′HA) are depicted in the *lower panel* by an anti-HA blot of total cellular lysates.

that for *E. coli* ClpA (48), and over 40-fold lower than the value for ClpB (50). While the basis of these differences is presently unclear, the resiliency of ClpX ATPase activity under conditions mimicking cellular stress (4) supports its membership in a Hsp100 class of stress tolerance proteins (6–9, 30, 45, 51).

The absence of multiple transcripts in all tissues but the testes and the direct correspondence of the ~2.9-kb cDNA, which we have cloned with the single ~2.9-kb transcript identified by Northern analysis, suggest the existence of a single form of ClpX in most tissues. Within this single transcript, the identification of two alternative start ATGs (M_1 and M_2) by *in vitro* transcription/translation experiments initially posed the exciting possibility that both mitochondrial and cytosolic forms of ClpX could be generated from the same transcript as has been documented for other proteins (52, 53). Such a mechanism for subcellular compartmentalization would be both biologically economical as well as resourceful, since it could provide a means of controlling differential compartmentalization in response to cellular metabolic status. However, GFP fusions with ClpXM$_1$ and ClpXM$_2$ both localized to the mitochondria and suggest that mice, like yeast, do not possess a cytosolic form of ClpX. Indeed, the truncated second form observed in the transcription/translation reactions may simply represent an aberrant product of the *in vitro* reaction.

The tissue-specific pattern of ClpX expression is inconsistent with a role as a constitutive chaperone and suggests that ClpX has acquired tissue-specific mitochondrial functions. The lack of an essential requirement of eukaryotic mitochondrial ClpX for general cell viability under normal growth conditions has been supported by the absence of an obvious phenotypic effect following disruption of the ClpX homolog in yeast (30). It is particularly interesting that mouse ClpX is most highly expressed in the liver where the mitochondria participate in numerous cell type-specific functions. These liver-specific mitochondrial processes include the oxidation of drugs and other toxic compounds, the formation of ketone bodies, the synthesis of components of fatty acid precursors, and the generation of critical components of the nitrogen metabolic pathway. Eluci-

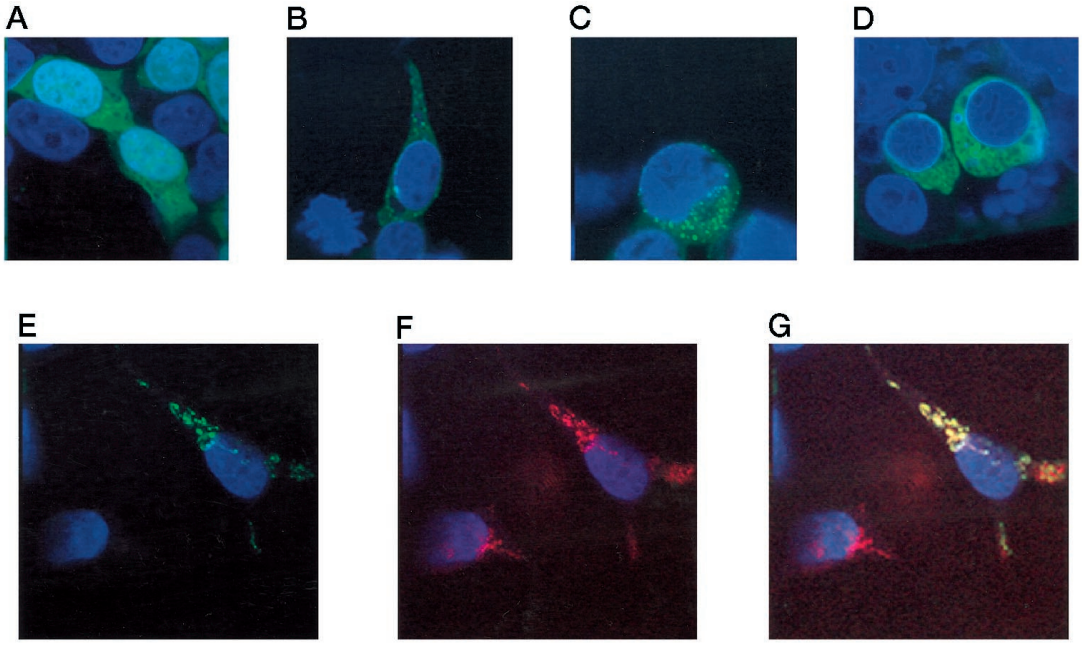

FIG. 7. **Subcellular localization of murine ClpX in transfected 293T cells using green fluorescent protein.** Serial N-terminal deletions of ClpX were overexpressed as fusions to the N terminus of enhanced green fluorescent protein (EGFP). The 293T cells were fixed and processed 24–36 h post-transfection and visualized by confocal laser-scanning microscopy. The nuclei in all panels are visualized by 4′,6′-diaminidino-2-phenylindole autofluorescence. Cells in *A* were transfected with EGFP alone. In *B* and *C*, ClpX-EGFP fusion proteins were initiated from either ATG 1 (pClpXM$_1$EGFP) or directly from ATG 2 (pClpXM$_2$EGFP), respectively. In *D*, the 65 N-terminal amino acids from the full-length preprotein were deleted, and translation was initiated by replacing the codon for alanine 66 with an ATG (pClpXΔ65EGFP). In *E–G*, pClpXEGFPM$_1$ was expressed in cells stained with the mitochondrial specific dye MitoTracker® Red CMXros. In *E*, the GFP fluorescence of ClpXM$_1$EGFP is demonstrated. The same field revealing MitoTracker staining is displayed in *F*, and co-localization of the two staining patterns is revealed in *G*.

dation of the cis-acting elements responsible for the varied pattern of basal tissue transcription and the characterization of potential stress response elements including the heat shock promoter element binding sites for heat shock transcription factors (54) awaits upcoming promoter analysis. Interestingly, the common regulatory mechanism governing expression of bacterial ClpX and ClpP (7), which are translated from a single transcript appears to be lost in humans where ClpX localizes to chromosome 15q22.2–22.3 and ClpP to chromosome 19q13. The divergent regulatory control is supported by the highly distinct pattern of ClpX and ClpP transcripts found in analogous tissues (this study and Ref. 30). Such divergence suggests that ClpX and ClpP may have acquired some independent cellular functions. However, the ability of ClpX and ClpP to function as part of a chaperone-protease system is still implied by their capacity to form a stable complex *in vivo*.

Identification of the eukaryotic targets of mouse ClpX may be informed by parallels with the bacterial system. *E. coli* ClpX binds to the C-terminal 7–11 amino acids of the Mu transposase (22), of the Mu repressor (24), of the SsrA C-terminal peptide tails (18), and of the *C. crescentus* cell-cycle regulator CtrA (21) through a direct interaction with the ClpX C-terminal PDZ domains (3). Although not highly conserved in amino acid sequence, this C-terminal targeting sequence (CTS) is characterized by a central charged core flanked by hydrophobic amino acids. Transfer of the CTS to heterologous proteins transforms them into substrates for *E. coli* ClpX function (22). Since the PDZ domains of mouse are approximately 60% similar to those of *C. elegans*, *S. cerevisiae*, and *E. coli*, it is highly plausible that the mode and targets of substrate recognition by ClpX will also be evolutionarily conserved. To identify eukaryotic mitochondrial proteins possessing a CTS homologous to that of MuA, the Mu repressor, SsrA proteins, or CtrA, we analyzed the mitochondrial subcategory of the Yeast Protein Data base (http://www.proteome.com/YPDhome.html) (55). Since this resource is a compilation of nearly all yeast mitochondrial genes as identified from the complete sequence of the yeast genome (29, 56), it provides a thorough representation of the entire range of potential ClpX substrates. Interestingly, of the 293 mitochondrial proteins in the data base, only nine fulfilled our criteria (see "Experimental Procedures") for homology to the CTS within the last 11 amino acids: electron transferring flavoprotein, β chain (GenBank™ accession number 1323371), citrate transport protein 1 (GenBank™ accession number 536746), import receptors of the outer membrane TOM70 and TOM72 (GenBank™ accession numbers 1302050 and 529136), RIP1 component of the cytochrome bc$_1$ complex (GenBank™ accession number 602391), NADH-ubiquinone oxidoreductase (GenBank™ accession number 805022), MSH1, the yeast homolog of *E. coli* MutS (GenBank™ accession number 529134), proline oxidase (GenBank™ accession number 1360564), and the E2 component of the pyruvate dehydrogenase complex (GenBank™ accession number 1301955). The first six potential substrates are in agreement with the tight inner membrane association observed for *S. cerevisiae* ClpX (30). This information, which suggests a possible role of ClpX in modulation of molecular import, electron transport, biochemical pathways and cell viability during normal or stressed cellular conditions, may ultimately prove valuable in elucidating its role in mammalian mitochondrial protein homeostasis.

Acknowledgments—We thank Zhen-Qiang Pan, Stuart Aaronson, and Patricia Cortes for their kind and generous guidance and support. We also thank Adolfo Garcia-Sastre, Ulrich Hermanto, Vassilis Aidinis, and Jose Trincao for their generous help and Larry Shapiro for critical review of the manuscript.

Addendum—A human homolog has been reported recently (GenBank™ accession number AJ006267 (C. Jespersgaard, P. Bross, T. J.

Corydon, B. S. Andresen, T. Kruse, L. Bolund, and N. Gregersen, unpublished data)).

REFERENCES

1. Schirmer, E. C., Glover, J. R., Singer, M. A., and Lindquist, S. (1996) *Trends Biochem. Sci.* **21,** 289–296
2. Beuron, F., Maurizi, M. R., Belnap, D. M., Kocsis, E., Booy, F. P., Kessel, M., and Steven, A. C. (1998) *J. Struct. Biol.* **123,** 248–259
3. Levchenko, I., Smith, C. K., Walsh, N. P., Sauer, R. T., and Baker, T. A. (1997) *Cell* **91,** 939–947
4. Schirmer, E. C., Queitsch, C., Kowal, A. S., Parsell, D. A., and Lindquist, S. (1998) *J. Biol. Chem.* **273,** 15546–15552
5. Schmitt, M., Neupert, W., and Langer, T. (1995) *EMBO J.* **14,** 3434–3444
6. Schmitt, M., Neupert, W., and Langer, T. (1996) *J. Cell Biol.* **134,** 1375–1386
7. Gottesman, S., Clark, W. P., de Crecy-Lagard, V., and Maurizi, M. R. (1993) *J Biol Chem* **268,** 22618–22626
8. Gerth, U., Wipat, A., Harwood, C. R., Carter, N., Emmerson, P. T., and Hecker, M. (1996) *Gene* (*Amst.*) **181,** 77–83
9. Gerth, U., Kruger, E., Derre, I., Msadek, T., and Hecker, M. (1998) *Mol. Microbiol.* **28,** 787–802
10. Kruklitis, R., Welty, D. J., and Nakai, H. (1996) *EMBO J.* **15,** 935–944
11. Levchenko, I., Luo, L., and Baker, T. A. (1995) *Genes Dev.* **9,** 2399–2408
12. Mhammedi-Alaoui, A., Pato, M., Gama, M. J., and Toussaint, A. (1994) *Mol. Microbiol.* **11,** 1109–1116
13. Wawrzynow, A., Wojtkowiak, D., Marszalek, J., Banecki, B., Jonsen, M., Graves, B., Georgopoulos, C., and Zylicz, M. (1995) *EMBO J.* **14,** 1867–1877
14. Kessel, M., Maurizi, M. R., Kim, B., Kocsis, E., Trus, B. L., Singh, S. K., and Steven, A. C. (1995) *J. Mol. Biol.* **250,** 587–594
15. Wang, J., Hartling, J. A., and Flanagan, J. M. (1997) *Cell* **91,** 447–456
16. Wojtkowiak, D., Georgopoulos, C., and Zylicz, M. (1993) *J. Biol. Chem.* **268,** 22609–22617
17. Schweder, T., Lee, K. H., Lomovskaya, O., and Matin, A. (1996) *J. Bacteriol.* **178,** 470–476
18. Gottesman, S., Roche, E., Zhou, Y., and Sauer, R. T. (1998) *Genes Dev.* **12,** 1338–1347
19. Lehnherr, H., and Yarmolinsky, M. B. (1995) *Proc. Natl. Acad. Sci. U. S. A.* **92,** 3274–3277
20. Domian, I. J., Quon, K. C., and Shapiro, L. (1997) *Cell* **90,** 415–424
21. Jenal, U., and Fuchs, T. (1998) *EMBO J.* **17,** 5658–5669
22. Levchenko, I., Yamauchi, M., and Baker, T. A. (1997) *Genes Dev.* **11,** 1561–1572
23. Geuskens, V., Mhammedi-Alaoui, A., Desmet, L., and Toussaint, A. (1992) *EMBO J.* **11,** 5121–5127
24. Laachouch, J. E., Desmet, L., Geuskens, V., Grimaud, R., and Toussaint, A. (1996) *EMBO J.* **15,** 437–444
25. Martin, J., and Hartl, F. U. (1997) *Curr. Opin. Struct. Biol.* **7,** 41–52
26. Martin, J. (1997) *J. Bioenerg. Biomembr.* **29,** 35–43
27. Hartl, F. U., and Neupert, W. (1990) *Science* **247,** 930–938
28. Schwartz, R. M., and Dayhoff, M. O. (1978) *Science* **199,** 395–403
29. Goffeau, A., Barrell, B. G., Bussey, H., Davis, R. W., Dujon, B., Feldmann, H., Galibert, F., Hoheisel, J. D., Jacq, C., Johnston, M., Louis, E. J., Mewes, H. W., Murakami, Y., Philippsen, P., Tettelin, H., and Oliver, S. G. (1996) *Science* **274,** 546
30. van Dyck, L., Dembowski, M., Neupert, W., and Langer, T. (1998) *FEBS Lett.* **438,** 250–254
31. Corydon, T. J., Bross, P., Holst, H. U., Neve, S., Kristiansen, K., Gregersen, N., and Bolund, L. (1998) *Biochem. J.* **331,** 309–316
32. Bross, P., Andresen, B. S., Knudsen, I., Kruse, T. A., and Gregersen, N. (1995) *FEBS Lett.* **377,** 249–252
33. Adams, M. D., Kelley, J. M., Gocayne, J. D., Dubnick, M., Polymeropoulos, M. H., Xiao, H., Merril, C. R., Wu, A., Olde, B., Moreno, R. F., *et al.* (1991) *Science* **252,** 1651–1656
34. Miki, T., Fleming, T. P., Bottaro, D. P., Rubin, J. S., Ron, D., and Aaronson, S. A. (1991) *Science* **251,** 72–75
35. Deloukas, P., Schuler, G. D., Gyapay, G., Beasley, E. M., Soderlund, C., Rodriguez-Tome, P., Hui, L., Matise, T. C., McKusick, K. B., Beckmann, J. S., Bentolila, S., Bihoreau, M., Birren, B. B., Browne, J., Butler, A., Castle, A. B., Chiannilkulchai, N., Clee, C., Day, P. J. R., Dehejia, A., Dibling, T., Drouot, N., Duprat, S., Fizames, C., Fox, S., *et al.* (1998) *Science* **282,** 744–746
36. Schuler, G. D., Boguski, M. S., Stewart, E. A., Stein, L. D., Gyapay, G., Rice, K., White, R. E., Rodriguez-Tome, P., Aggarwal, A., Bajorek, E., Bentolila, S., Birren, B. B., Butler, A., Castle, A. B., Chiannilkulchai, N., Chu, A., Clee, C., Cowles, S., Day, P. J., Dibling, T., Drouot, N., Dunham, I., Duprat, S., East, C., Hudson, T. J., and *et al.* (1996) *Science* **274,** 540–546
37. Spanopoulou, E., Cortes, P., Shih, C., Huang, C. M., Silver, D. P., Svec, P., and Baltimore, D. (1995) *Immunity* **3,** 715–726
38. Spanopoulou, E., Zaitseva, F., Wang, F. H., Santagata, S., Baltimore, D., and Panayotou, G. (1996) *Cell* **87,** 263–276
39. Raynes, D. A., and Guerriero, V., Jr. (1998) *J. Biol. Chem.* **273,** 32883–32888
40. Walker, J. E., Saraste, M., and Gay, N. J. (1982) *Nature* **298,** 867–869
41. Claros, M. G., and Vincens, P. (1996) *Eur. J. Biochem.* **241,** 779–786
42. Gavel, Y., and von Heijne, G. (1990) *Protein Eng.* **4,** 33–37
43. Roise, D., and Schatz, G. (1988) *J. Biol. Chem.* **263,** 4509–4511
44. Saraste, M., Sibbald, P. R., and Wittinghofer, A. (1990) *Trends Biochem. Sci.* **15,** 430–434
45. Sanchez, Y., and Lindquist, S. L. (1990) *Science* **248,** 1112–1115
46. Sanchez, Y., Taulien, J., Borkovich, K. A., and Lindquist, S. (1992) *EMBO J.* **11,** 2357–2364
47. Szabo, A., Korszun, R., Hartl, F. U., and Flanagan, J. (1996) *EMBO J.* **15,** 408–417
48. Hwang, B. J., Woo, K. M., Goldberg, A. L., and Chung, C. H. (1988) *J. Biol. Chem.* **263,** 8727–8734
49. Katayama-Fujimura, Y., Gottesman, S., and Maurizi, M. R. (1987) *J. Biol. Chem.* **262,** 4477–4485
50. Woo, K. M., Kim, K. I., Goldberg, A. L., Ha, D. B., and Chung, C. H. (1992) *J. Biol. Chem.* **267,** 20429–20434
51. Leonhardt, S. A., Fearson, K., Danese, P. N., and Mason, T. L. (1993) *Mol. Cell. Biol.* **13,** 6304–6313
52. Attardi, G., and Schatz, G. (1988) *Annu. Rev. Cell Biol.* **4,** 289–333
53. Land, T., and Rouault, T. A. (1998) *Mol. Cell* **2,** 807–815
54. Morimoto, R. I. (1998) *Genes Dev.* **12,** 3788–3796
55. Hodges, P. E., Payne, W. E., and Garrels, J. I. (1998) *Nucleic Acids Res.* **26,** 68–72
56. Goffeau, A., Barrell, B. G., Bussey, H., Davis, R. W., Dujon, B., Feldmann, H., Galibert, F., Hoheisel, J. D., Jacq, C., Johnston, M., Louis, E. J., Mewes, H. W., Murakami, Y., Philippsen, P., Tettelin, H., and Oliver, S. G. (1996) *Science* **274,** 563–567